

5-2-2009

Polarity-Related Asymmetry At ZnO Surfaces and Metal interfaces

Y. F. Dong

Z-Q. Fang

David C. Look

Wright State University - Main Campus, david.look@wright.edu

Daniel R. Douth

M. J. Hetzer

See next page for additional authors

Follow this and additional works at: <https://corescholar.libraries.wright.edu/physics>



Part of the [Physics Commons](#)

Repository Citation

Dong, Y. F., Fang, Z., Look, D. C., Douth, D. R., Hetzer, M. J., & Brillson, L. J. (2009). Polarity-Related Asymmetry At ZnO Surfaces and Metal interfaces. *Journal of Vacuum Science & Technology B*, 27 (3), 1710-1716.
<https://corescholar.libraries.wright.edu/physics/5>

This Article is brought to you for free and open access by the Physics at CORE Scholar. It has been accepted for inclusion in Physics Faculty Publications by an authorized administrator of CORE Scholar. For more information, please contact corescholar@www.libraries.wright.edu, library-corescholar@wright.edu.

Authors

Y. F. Dong, Z-Q. Fang, David C. Look, Daniel R. Douth, M. J. Hetzer, and L. J. Brillson

Polarity-related asymmetry at ZnO surfaces and metal interfaces

Yufeng Dong^{a)}

Department of Electrical and Computer Engineering, The Ohio State University, Columbus, Ohio 43210

Z.-Q. Fang and D. C. Look

Semiconductor Research Center, Wright State University, Dayton, Ohio 45435

D. R. Douth and M. J. Hetzer

Department of Physics, The Ohio State University, Columbus, Ohio 43210

L. J. Brillson

Department of Electrical and Computer Engineering, The Ohio State University, Columbus, Ohio 43210;

Department of Physics, The Ohio State University, Columbus, Ohio 43210; and Center for Materials

Research, The Ohio State University, Columbus, Ohio 43210

(Received 8 December 2008; accepted 23 March 2009; published 29 May 2009)

Clean ZnO (0001) Zn- and (000 $\bar{1}$) O-polar surfaces and metal interfaces have been systematically studied by depth-resolved cathodoluminescence spectroscopy, photoluminescence, current-voltage and capacitance-voltage measurements, and deep level transient spectroscopy. Zn-face shows higher near band edge emission and lower near surface defect emission. Even with remote plasma decreases of the 2.5 eV near surface defect emission, (0001)-Zn face emission quality still exceeds that of (000 $\bar{1}$)-O face. The two polar surfaces and corresponding metal interfaces also present very different luminescence evolution under low-energy electron beam irradiation. Ultrahigh vacuum-deposited Au and Pd diodes on as-received and O₂/He plasma-cleaned surfaces display not only a significant metal sensitivity but also a strong polarity dependence that correlates with defect emissions, traps, and interface chemistry. Pd diode is always more leaky than Au diode due to the diffusion of H, while Zn-face is better to form Schottky barrier for Au compared with O-face. A comprehensive model accounts for the metal-and polarity-dependent transport properties. © 2009 American Vacuum Society. [DOI: 10.1116/1.3119681]

I. INTRODUCTION

As one of the most important candidates for next generation semiconductor devices, ZnO has been studied extensively in recent years.¹ Although metal/ZnO interfaces are essential to all ZnO electronic device applications, it still remains a challenge to fabricate high quality and thermally stable ZnO contacts. Their electronic properties have only recently been explored in detail.²⁻⁷ The famous Schottky-Mott theory is seldom obeyed by metals on ZnO, i.e., their Schottky barrier heights are not proportional to their work functions.⁸ Our previous studies revealed the importance of surface and near surface effects, including surface adsorbates, near-interface native defects, interface chemical bonding, and thermally induced interface chemical interactions at metal/ZnO contacts.^{3,9-12} Now, we are correlating polarity-related surface and near surface defects and chemical reactions with electronic properties.¹³ Surface polarity plays important role in wurtzite semiconductor devices. Significant polarity-related effects have been found in GaN-based devices.¹⁴ Likewise, homoepitaxial ZnO layers grown on polar surfaces have very different optical properties and impurity levels.¹⁵ The stabilization mechanisms of Zn(0001)- or O(000 $\bar{1}$)-terminated faces have been a source of controversy for quite some time.¹⁶ Differences between hydrothermal

ZnO polar surfaces were ascribed to surface band bending induced by spontaneous polarization,¹⁷ while melt-grown ZnO exhibits only a small difference in band bending.¹⁸ However, it is still not clear which polar face should give better Schottky contacts because few comparisons between two polarities exist regarding their surface optical properties, defect concentrations, metal reactivities with various metal contacts, and Schottky barrier heights.

In this study, we probed the polarity- and metal-dependent properties of (0001) Zn- and (000 $\bar{1}$) O-polar surfaces of single crystalline ZnO with very low bulk defect grown by vapor phase process and their metal contacts by using nanoscale depth-resolved cathodoluminescence spectroscopy (DRCLS) coupled with surface science and electronic transport techniques.

II. EXPERIMENT

Vapor-phase grown single crystal ZnO samples from ZN Technology Inc. and polished chemomechanically on both the (0001) and (000 $\bar{1}$) faces had mid-10¹⁶ cm⁻³ carrier concentration and 220 cm²/V s Hall mobility at 300 K.¹⁹ All samples were ultrasonically cleaned in acetone, dimethylsulfoxide, methanol, isopropyl alcohol, and de-ionized water for 5 min, respectively, then nitrogen blow dried. These samples are referred as "as-received." We used remote oxygen plasma (ROP) treatment to remove surface adsorbates and subsurface impurities and defects such as oxygen

^{a)} Author to whom correspondence should be addressed; electronic mail: dong.70@osu.edu

vacancies.^{2,3} For the plasma-cleaned samples, both Zn- and O-faces from separate halves of the same as-received ZnO crystal were ROP processed for 1–2 h. Subsequent atomic force microscopy measurements show only negligible increase in surface roughness. In general, the Zn-face is smoother than O-face (rms 0.2 nm versus 0.4 nm) although both surfaces have very smooth surfaces. Both surfaces show no atomic step edges, grain boundaries, or polishing scratches, no matter ROP cleaned or not. Arrays of metal diodes (Au, Pd, and Ta, 0.4 mm diameter, 30 nm thick) were e-beam deposited *in situ* on two ROP-cleaned and as-received polar surfaces at mid- 10^{-9} Torr pressures. We note the importance of *in situ* metal deposition on clean surfaces within the same plasma chamber. It has been recognized that ZnO surfaces are very reactive even under atmosphere. The surface adsorbates (primarily OH^-) will form a surface conductive layer, degrade metal contacts, and introduce Schottky barrier diode (SBD) leakage. The UHV e-beam deposition was kept at a slow rate (~ 1 nm/min) to avoid possible metal-deposition-induced surface damage. Subsequently, we prepared Ohmic contacts on the entire back side of each ZnO piece using e-beam deposited (40/60/30 nm) Ti/Ni/Au film. DRCLS, remote O_2/He plasma (ROP) processing, and deep level transient spectroscopy (DLTS) are described elsewhere.^{3,20}

III. RESULTS AND DISCUSSION

Figures 1(a) and 1(b) show DRCL spectra for as-received and 2 h ROP-treated Zn- and O-faces, respectively. Electron beam energies E_B varied from 1 to 5 keV, corresponding to depths U_0 of peak electron-hole pair creation rates increasing from 10 to 100 nm, respectively. Although spectral features appear similar, the Zn face displays four times higher band edge (NBE, at 3.45 eV) emission throughout the near surface region. ROP does not change the spectral features. Defect emission is always dominated by the 2.5 eV “green” emissions and no apparent new defect emission appears after 2 h ROP. Figure 2 shows relative defect intensity changes versus depth. The CL intensities (I_D or I_{NBE}) were read from their maximum peak values. Defect intensities are normalized relative to NBE intensities. The general trend of I_D/I_{NBE} decrease from surface indicates more oxygen vacancy defects in the surface region. The 2.5 eV green defect (I_D) and 3.45 eV near band edge (I_{NBE}) emission intensity exhibit significant polarity-related differences. The O face has two times higher defect intensity than the Zn face even after ROP cleaning. As-received surfaces show similar polarity effects. Figure 2 also shows that ROP cleaning effectively decreases the O-face I_D/I_{NBE} ratio, while changing the Zn-face ratio only slightly. We previously assigned the 2.5 eV peak to defects related to oxygen vacancies.⁹ The results indicate that the O-face has *more* oxygen vacancies than the Zn-face.

In cathodoluminescence measurements, we found a complex polarity- and metal-dependent luminescence evolutions under low electron beam irradiation of our scanning electron microscope. Electron beams with 2 and 5 kV energy were applied to bare surfaces and metal diodes, respectively,

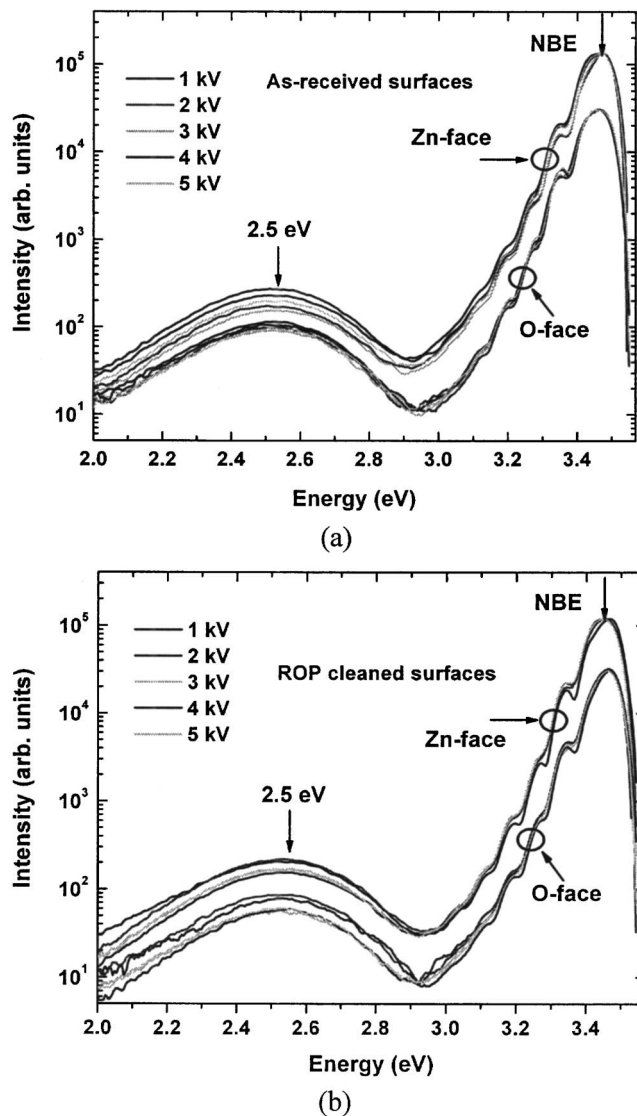


FIG. 1. DRCL spectra for (a) as-received Zn- and O-face (b) ROP cleaned Zn- and O-faces.

which give the same probing depth in ZnO (~ 24 nm). Figure 3 shows the time dependence of NBE emission for bare Zn- and O-face and their diodes. For Zn-face, the NBE intensity first increases slightly and then changes little after 50 s exposure. However, the O-face behaves very different, decreasing sharply by a factor of 6 at the first 100 s exposure. Similar polarity effects were found for hydrothermally grown ZnO single crystal samples, where the decrease in NBE intensity was attributed to metastable bulk defect reactions.²¹ It is reasonable that O-face, with much more defects, shows the sharp decrease in NBE intensity. The time dependence of NBE intensity for metal diodes on two polar surfaces is more complicated. There are two important features: (i) For Au diode, the NBE intensity is stable on the Zn-face while on the O-face, it is stable only for ~ 60 s, decreasing exponentially thereafter; and (ii) for Pd diodes, the intensity increases on the Zn-face while it increases slightly and then exponentially decreases on the O-face. The

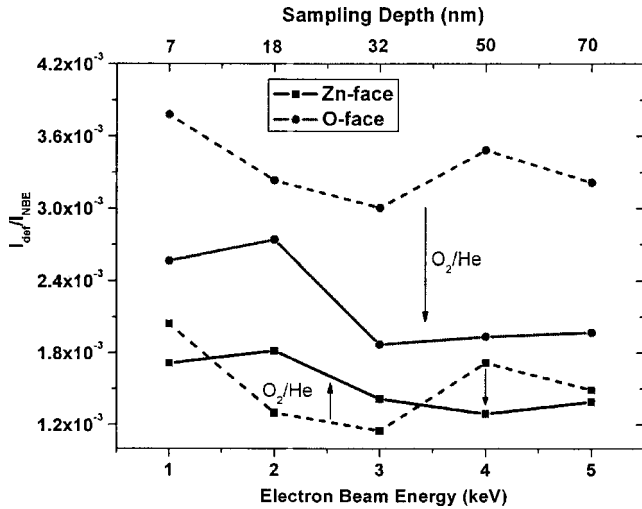
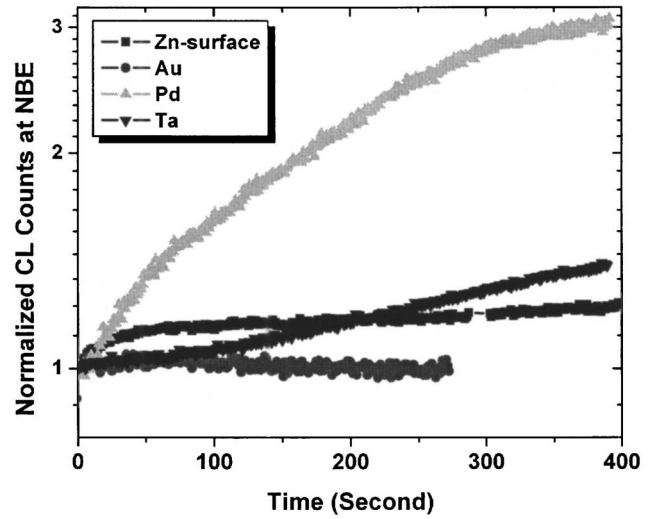


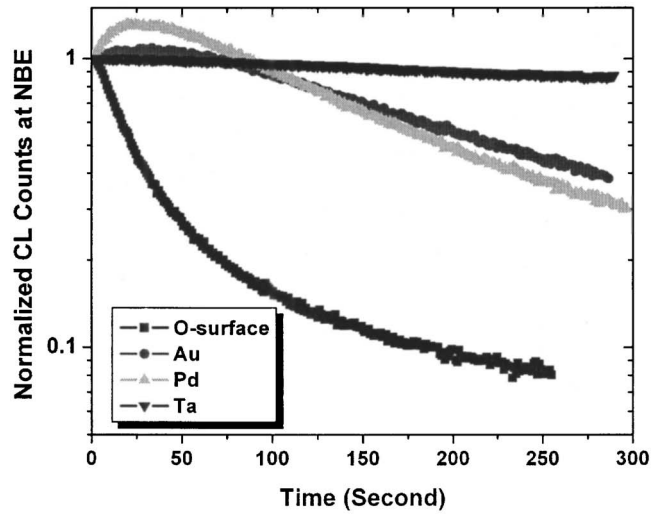
Fig. 2. Relative defect intensity changes vs depth for (0001) Zn and (000 $\bar{1}$) O faces.

mechanisms for the complicated electron-beam-irradiation-induced processes are related not only to the metastable near surface defects induced by e-beam but also to the metal/ZnO interface chemistry, which are still under investigation. Nevertheless, the different behavior of Zn- and O-face shows the polarity effects and serves as a signature for two polar surfaces. We note that the DRCL spectra in Figs. 1 and 2 were recorded by a charge coupled device detector with 0.2 s e-beam exposure, where the mentioned time dependence is negligible.

The higher I_D of 2.5 eV defects in cathodoluminescence spectroscopy, previously associated with O vacancies,^{9,10} induces different transport behavior on the O- versus Zn-face-metal diodes. All the metal diodes (Au, Pd, and Ta) deposited on as received surfaces are Ohmic and there is an Ohmic to rectifying transition for Au and Pd diodes on ROP surfaces. However, electrical properties show both metal and polarity dependence. First, resistivity of two Au Ohmic contacts on the Zn-face increases monotonically while that on O-face decreases slightly as temperature decreases from 300 to 100 K, as shown in Fig. 4. This indicates more near surface defects at the O face than at the Zn face, consistent with the DRCLS results. Since gold contacts on as-received O-faces are Ohmic, the decrease in resistance with decreasing temperature is due to a mobility increase in bulk ZnO, assuming constant carrier concentration. The effects of vacuum activated layers, observed on highly resistive, compensated ZnO crystals,^{22,23} may not play the dominant role here. However, gold contacts on the Zn-face are not good Ohmic contacts even though their resistance is still low. Actually, the measured gold diodes can be viewed as two back-to-back poor Schottky diodes. Thus, we see the increase in resistance with decreasing temperature. In addition, subsequent ROP treatment through the diodes changes only the Au diodes on the Zn face from Ohmic to rectifying, indicating different chemistry for oxygen plasma on the two polar surfaces.



(a)



(b)

Fig. 3. CL time dependence of NBE emissions for Zn- and O-faces and their metal diodes.

For Au and Pd SBDs on ROP-treated surfaces, typical I - V characteristics at 300 K in Fig. 5 show not only metal sensitivity but also a polarity dependence. In general, Au/Zn-face SBDs have ten times lower leakage current and higher rectification than Au/O-face SBDs. Pd SBDs always have larger currents than Au SBDs in the entire bias region, with Pd on the Zn face the highest. The Pd/ZnO diode on the Zn-face shows forward current bending at lower biases and seems to have a higher series resistance. Actually, this is due to higher leakage currents at both reverse and forward biases. The leakage currents might be related to field-enhanced localized current paths.¹² Assuming that thermionic emission (TE) dominates forward current, then for $V > 3kT/q$, the current is $I = I_S \{ \exp[q(V - IR_S)/\eta kT] - 1 \}$, with $I_S = AA^*T^2 \exp(-q\Phi_{SB}^{IV}/kT)$ the saturation current, R_S the series resistance, η the ideality factor, A the diode area ($1.25 \times 10^{-3} \text{ cm}^2$), A^* the effective Richardson constant

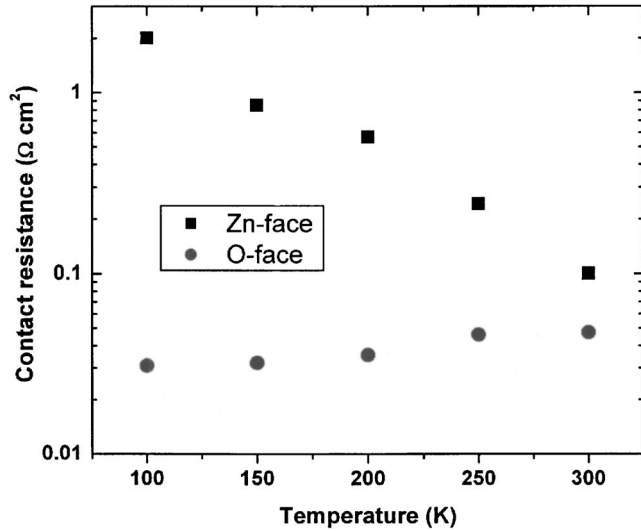


FIG. 4. Temperature-dependent contact resistances for two gold diodes on the Zn-or O-faces.

($32 \text{ A cm}^{-2} \text{ K}^{-2}$), and $\Phi_{\text{SB}}^{\text{IV}}$ the zero-biased SBH. Ideality factor η and effective barrier heights from a TE model are summarized in Table I. Au SBDs have larger Schottky barrier height than Pd SBDs, notwithstanding the same work function values.²⁴ Furthermore, the very different SBD behavior for the same metal, either Au or Pd, on the Zn- or O-face indicates strong polarity effects. Note that the TE model alone cannot account for the large reverse currents, especially for Pd SBDs, where defect-assisted tunneling and/or hopping may play a role. Therefore, the barrier height evaluated from I - V for Pd SBDs may not be as accurate as that for Au SBDs. The nonideal characteristic of Au and Pd diodes may also be attributed to the inhomogeneous Schottky barriers.^{25,26} Temperature-dependent I - V characteristics for Au/ZnO and Pd/ZnO SBDs will be reported elsewhere.³⁰

We have carried out C^{-2} - V measurements at 1 MHz, 100 kHz, and 10 kHz. Figure 6 shows the room temperature C^{-2} - V characteristics at 1 MHz for the same Au- and Pd-SBDs. The frequency dependence is negligible. Due to the small series resistance ($R_S, \sim 50 \Omega$) for both Au and Pd SBDs, the criterion $R_S \ll (\omega C)^{-1}$ for the accurate determination of depletion capacitance can be satisfied at all frequencies. $\Phi_{\text{SB}}^{\text{CV}}$ values were calculated from $\Phi_{\text{SB}}^{\text{CV}} = V_i + V_0 + kT/q$ with V_i the intercept and $V_0 = (kT/q) \ln(N_C/N_D)$.²⁷ Note that C^{-2} - V characteristics are linear only for O-face SBDs and they bend down for SBDs on the Zn-face when approaching

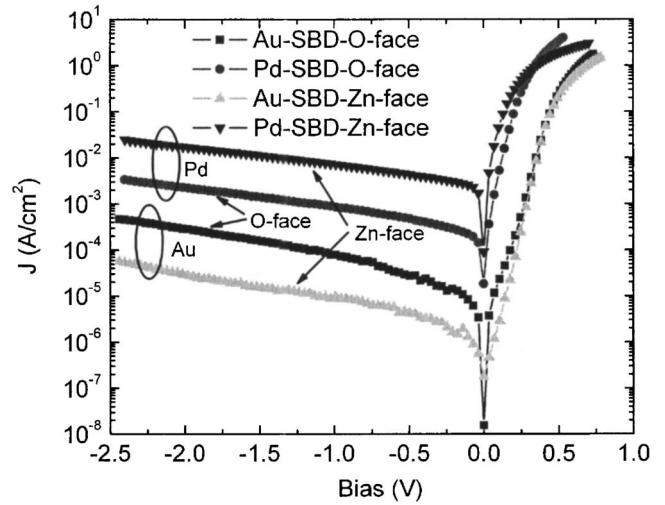


FIG. 5. Typical I - V characteristics at 300 K for Au and Pd SBDs on ROP treated Zn- and O-faces.

zero bias, which indicates the carrier inhomogeneity for Zn-face with depth. Table I shows $\Phi_{\text{SB}}^{\text{CV}}$ values for the SBDs extracted by linear fitting, which confirms the better rectifying behavior of Au than Pd SBDs. The evaluated $\Phi_{\text{SB}}^{\text{CV}}$ values are larger than $\Phi_{\text{SB}}^{\text{IV}}$, especially for Au diodes, indicating the lateral inhomogeneity. The associated carrier density profiles as shown in Fig. 7 are strongly polarity- and metal dependent. There are two important features: (i) net carrier concentrations ($N_d - N_a = N_{\text{eff}}$) are constant for both the Au and Pd SBDs on the O-face in the near surface region (90–170 nm), whereas they gradually decrease by about 30% in the same region for Au and Pd on the Zn-polar surface; and (ii) N_d increases sharply for the Pd SBDs on both polar surfaces at the shallowest depths profiled by C - V . Similar decrease in surface carrier concentration was also found for Pt diodes on sulfide treated ZnO O faces²⁸ and for Pd on hydrogen peroxide treated ZnO O faces.⁶ But this is the first report of the polarity dependence for ROP cleaned surfaces. Note that due to higher currents at zero bias on Pd/ZnO diodes, as compared to Au/ZnO diodes, larger conductance is involved in the capacitance measurement, which may contribute to the sharp increase in carrier concentration at near surface region. Nevertheless, large conductance and sharp increase in N_d indicate a surface conductive layer at Pd/ZnO interfaces.

The observed decrease in carrier concentration at the near surface region of Zn-face is closely related to oxygen plasma treatment, which further decreases toward the surface with

TABLE I. SBD characteristics at 300 K for Pd and Au on Zn- and O-polar surfaces.

Surface	Schottky metal	Ideality η	$\Phi_{\text{SB}}^{\text{IV}}$ (eV)	$\Phi_{\text{SB}}^{\text{CV}}$ (eV)	$N_d - N_a$ ($\times 10^{17} \text{ cm}^{-3}$)
(0001) Zn	Au	1.2	0.81	1.20	0.7–1.0
(0001) Zn	Pd	1.3	0.53	0.73	0.8–1.0
(000 $\bar{1}$) O	Au	1.3	0.77	1.07	1.1
(000 $\bar{1}$) O	Pd	1.2	0.61	0.68	1.1

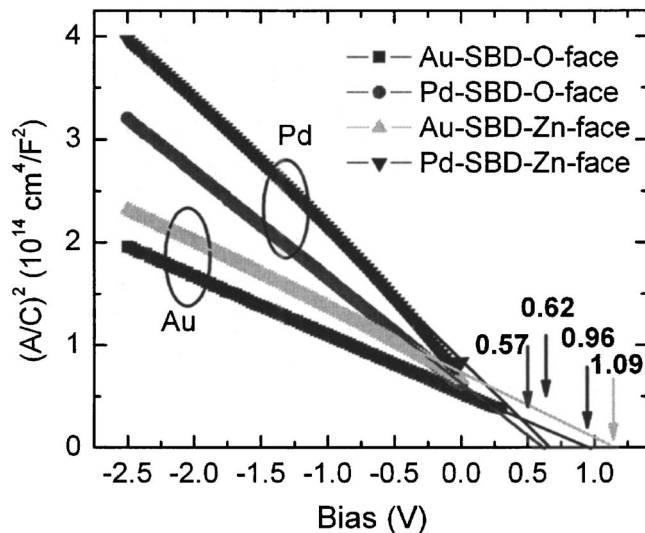


FIG. 6. Typical $1/C^2$ - V curves at 300 K for Au- and Pd-SBDs on ROP treated Zn- and O-faces.

increasing ROP time, while that at the O-face is independent of ROP time. The oxygen plasma is much more likely to react with the Zn-face than with the O-face. Because there is no obvious new defect CL emission other than the 2.5 eV emission (due to oxygen vacancy) after up to 2 h ROP, the possibility of Zn vacancy formation (as deep acceptor) can be excluded, since Zn vacancy-related defects should have an emission peak around 2.1 eV if present.⁹ Hydrogen removal from surface regions can also decrease the carrier profile by decreasing donor density or activating acceptor impurities. Conversely, a previous study found that remote hydrogen plasma treatment increased surface electron concentration in single crystal ZnO.²⁹ Consistent with hydrogen removal, recent 4.2 K PL shows that ROP reduces the I_4 line at 3.368 eV assigned to hydrogen donor bound exciton on the Zn-face but much less on the O-face for the same samples.³⁰ First principles calculations provide further evidence that it is much easier for hydrogen to diffuse out of the Zn face.³¹ However, there is no asymmetry for oxygen diffusion within ZnO.³² Therefore, we propose several points about the polarity-related ROP effects: (i) ROP cleans both surfaces by removing surface adsorbates; (ii) ROP effectively removes hydrogen from the Zn face and dissociates V_O -H complexes within the near surface region; (iii) ROP decreases V_O density on the O face, which was shown by the decrease in CL defect emission, but have no effect on the carrier profile as V_O is a deep level; and (iv) ROP can also decrease V_O density on the Zn face, although the decrease in free carrier density is dominated by the dissociation of V_O -H complexes. Thus, while ROP removes O vacancies and H from both surfaces, the higher O vacancy concentration and lower H removal rate at the O surface result in higher near surface carrier concentrations at the O face.

ZnO has strong spontaneous polarization along the $\langle 0001 \rangle$ direction, which can induce electron accumulation/depletion on the ideal O/Zn faces and make n -type SBDs easier to form on the Zn face.^{17,33} However, metal diodes on as-

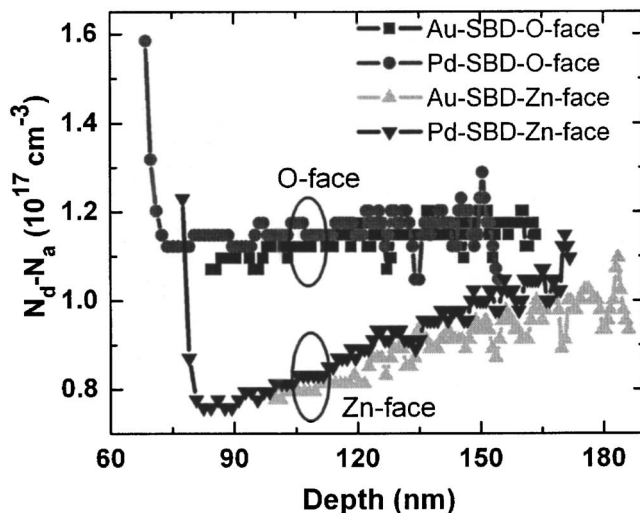


FIG. 7. Near surface carrier-concentration profiles for Au- and Pd-SBDs on ROP treated Zn- and O-faces.

received Zn and O faces are Ohmic which indicates electron accumulation on both surfaces due to surface adsorbates. ROP can effectively remove surface adsorbates. But it is difficult to stabilize the ideal Zn face in an O-rich atmosphere.¹⁶ Therefore, we argue that spontaneous polarization is not the dominant role that decides the polarity effects found here.

With increasing ROP time from 1 to 2 h, the SBDs' rectification increases, regardless of the surface polarity. But the polarity dependence and metal sensitivity are still significant. Our DLTS reveals the evolution of defect traps with ROP time. E3 is the dominant trap for all SBDs. It is closely related to ROP, increasing with ROP exposure time on both surfaces but only shifting in energy on the Zn face. One surface trap E5 was only found for Pd SBD on 1 h ROP cleaned Zn-face, consistent with DRCL results.¹² The detailed DLTS results will be reported elsewhere.³⁰

The surface conductive layer at Pd/ZnO interfaces is due to hydrogen diffusion. It is easy for hydrogen to penetrate the thin Pd film and accumulate at interfaces. Our PL data indicate that this accumulation is larger for the Zn-face. Figure 8 shows low temperature (80 K) PL spectra for ROP treated bare Zn-face, Pd, and Au SBDs. Pd SBDs exhibit a much larger I_4 peak increase, compared with Au SBDs. Pd SBDs exhibit a similar enhancement on the O-face but in smaller magnitude. Interface H^+ acts as donors, forms negative interface dipole with its image charge on the metal side, and decreases Schottky barriers at Pd/ZnO interfaces. We calculated the interface Fermi level position as a function of H-related surface donor density, as shown in Fig. 9. In Schottky limit, barrier height is given by the energy difference of metal work function (Φ_M) and semiconductor electron affinity (EA), while in Bardeen limit the interface Fermi level is pinned close to the defect level. ZnO has an EA around 4.0–4.4 eV, depending on surface properties. With a negative interface dipole ΔV , the Schottky barrier height Φ_B

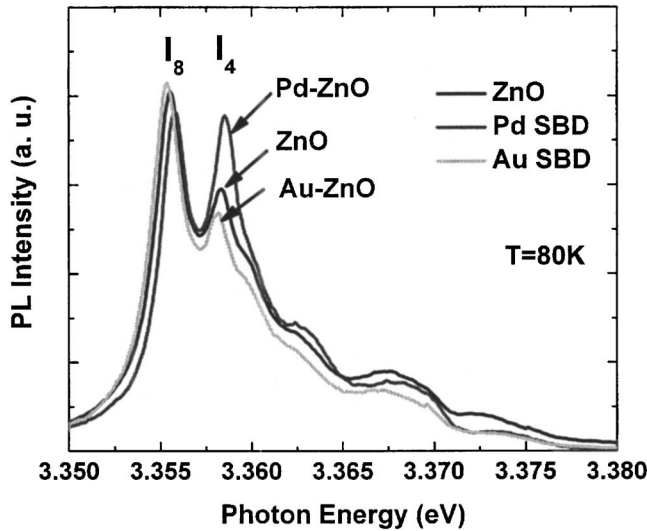


FIG. 8. 80 K PL for ZnO surfaces and Pd/Au SBDs.

is given by $\Phi_B = \Phi_M - EA - |\Delta V|$. As shown by Fig. 9, Schottky barrier is reduced by ~ 0.4 eV with $10^{13}/\text{cm}^2$ surface donor density.

To account for these metal- and polarity-dependent carrier concentration profiles, we propose a comprehensive model and describe the effective donor concentration N_d^{eff} as

$$N_d^{\text{eff}} = N_d^{\text{bulk}} + N_d^{\text{surf}} \exp(-z/d_1) - N_a^{\text{surf}} \exp(-z/d_2), \quad (1)$$

where N_d^{bulk} is the bulk donor concentration and N_d^{surf} and N_a^{surf} are surface donor and acceptor densities decaying away from the surface with decay lengths d_1 and d_2 , respectively. The sharp N_d increase for Pd SBDs near the surface is due to hydrogen incorporation at the interface and it is consistent with the most leaky I - V characteristic for Pd SBDs on the Zn-face. The N_d^{surf} term describes the sharp N_d^{eff} increase within the outer few nanometers due to H and perhaps to impurity segregation from the bulk.³⁴ A N_a^{surf} surface acceptor term with $d_2 \sim 100$ nm accounts for the Zn-face N_d^{eff} subsurface decrease, possibly due to the polarity-dependent

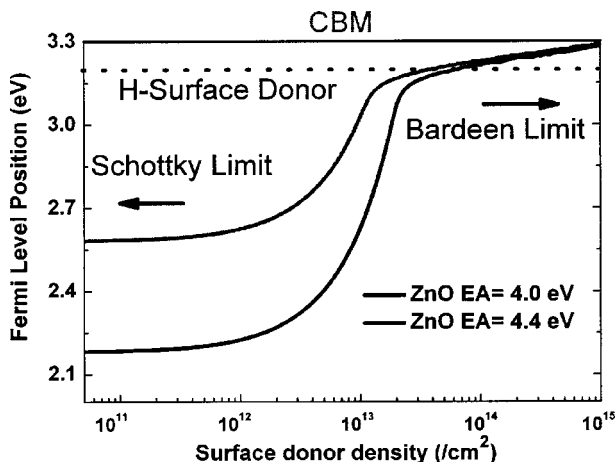


FIG. 9. Calculated interface Fermi level as a function of surface H^+ donor density.

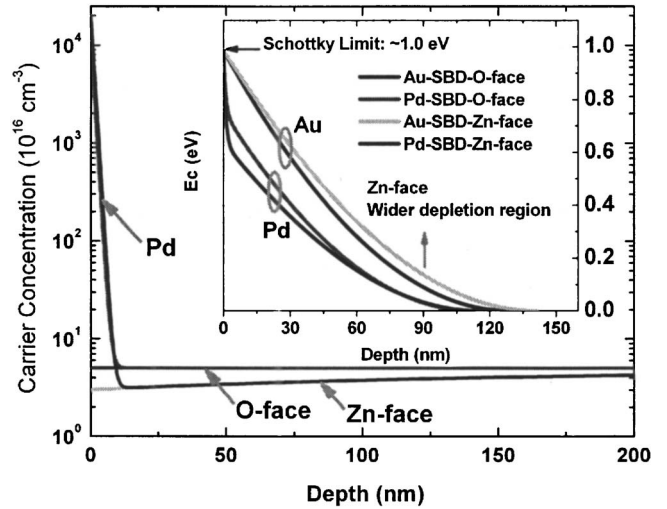


FIG. 10. Carrier concentration profiles and calculated conduction band diagrams for Au and Pd SBDs on the Zn- and O-faces.

H-removal. With reasonable values assigned to the terms in Eq. (1) and by solving Poisson's equations, the carrier profile and associated conduction band diagram are shown in Fig. 10. The rapidly increasing N_d^{eff} near the Pd/ZnO (0001) and (000 $\bar{1}$) interfaces narrows the surface space charge region and forms an ultrathin surface barrier, which also represents the negative interface dipole ΔV . Thus tunneling through a hydrogen-induced interface dipole decreases the effective Schottky barrier. In addition, introduction of N_d^{surf} widens the SBDs' depletion region on the Zn versus O-face. The revised band bending is consistent with the Table I values of $\Phi_{\text{SB}}^{\text{CV}}$ and $\Phi_{\text{SB}}^{\text{IV}}$ and accounts for the metal and polarity dependences.

IV. CONCLUSION

The polarity-related asymmetry in ZnO c -plane polar surfaces and metal diodes has been studied by DRCLS and electrical measurements. Significant optical polarity signatures have been found for the Zn- and O-faces in CL, including higher oxygen vacancy density and faster evolution with exposure time on the O face. Au and Pd diodes on as-received and O_2/He plasma-cleaned surfaces display not only a significant metal sensitivity but also a strong polarity dependence that correlates with defect emissions, traps, and interface chemistry.

ACKNOWLEDGMENT

The authors gratefully acknowledge support from the National Science Foundation Grant No. DMR-0513968 (Verne Hess).

¹S. J. Pearton, D. P. Norton, K. Ip, Y. W. Heo, and T. Steiner, Prog. Mater. Sci. **50**, 312 (2005).

²B. J. Coppa, R. F. Davis, and R. J. Nemanich, Appl. Phys. Lett. **82**, 400 (2003).

³H. L. Mosbacker, Y. M. Strzhemechny, B. D. White, P. E. Smith, D. C. Look, D. C. Reynolds, C. W. Litton, and L. J. Brillson, Appl. Phys. Lett. **87**, 012102 (2005).

- ⁴M. W. Allen, M. M. Alkaisi, and S. M. Durbin, *Appl. Phys. Lett.* **89**, 103520 (2006).
- ⁵M. W. Allen and S. M. Durbin, *Appl. Phys. Lett.* **92**, 122110 (2008).
- ⁶R. Schifano, E. V. Monakhov, U. Grossner, and B. G. Svensson, *Appl. Phys. Lett.* **91**, 193507 (2007).
- ⁷Q. L. Gu *et al.*, *J. Appl. Phys.* **103**, 093706 (2008).
- ⁸K. Ip, G. T. Thaler, H. Yang, S. Y. Han, Y. Li, D. P. Norton, S. J. Pearton, S. Jang, and F. Ren, *J. Cryst. Growth* **287**, 149 (2006).
- ⁹L. J. Brillson *et al.*, *Appl. Phys. Lett.* **90**, 102116 (2007).
- ¹⁰H. L. Mosbacker *et al.*, *Appl. Phys. Lett.* **91**, 072102 (2007).
- ¹¹Y. Dong and L. J. Brillson, *J. Electron. Mater.* **37**, 743 (2008).
- ¹²Z.-Q. Fang, B. Claffin, D. C. Look, Y. F. Dong, H. L. Mosbacker, and L. J. Brillson, *J. Appl. Phys.* **104**, 063707 (2008).
- ¹³Y. Dong, Z.-Q. Fang, D. C. Look, G. Cantwell, J. Zhang, J. J. Song, and L. J. Brillson, *Appl. Phys. Lett.* **93**, 072111 (2008).
- ¹⁴L. K. Li, M. J. Jurkovic, W. I. Wang, J. M. Van Hove, and P. P. Chow, *Appl. Phys. Lett.* **76**, 1740 (2000).
- ¹⁵S. Lautenschlaeger, J. Scann, N. Volbers, B. K. Meyer, A. Hoffmann, U. Haboek, and M. R. Wagner, *Phys. Rev. B* **77**, 144108 (2008).
- ¹⁶C. Woll, *Prog. Surf. Sci.* **82**, 55 (2007).
- ¹⁷M. W. Allen, P. Miller, R. J. Reeves, and S. M. Durbin, *Appl. Phys. Lett.* **90**, 062104 (2007).
- ¹⁸S. A. Chevtchenko, J. C. Moore, Ü. Özgür, X. Gu, A. A. Baski, H. Morkoç, B. Nemeth, and J. E. Nause, *Appl. Phys. Lett.* **89**, 182111 (2006).
- ¹⁹D. C. Look, *Mater. Res. Soc. Symp. Proc.* **957**, 127 (2007).
- ²⁰D. C. Look and Z.-Q. Fang, *Appl. Phys. Lett.* **79**, 84 (2001).
- ²¹B. Dierre, X. L. Yuan, and T. Sekiguchi, *J. Appl. Phys.* **104**, 043528 (2008).
- ²²M. Allen *et al.*, *Mater. Res. Soc. Symp. Proc.* **1035**, L10-06 (2008).
- ²³O. Schmidt, A. Geis, P. Kiesel, C. G. V. de Walle, N. M. Johnson, A. Bakin, A. Waag, and G. H. Dohler, *Superlattices Microstruct.* **39**, 8 (2006).
- ²⁴H. B. Michaelson, *J. Appl. Phys.* **48**, 4729 (1977).
- ²⁵H. Sheng, S. Muthukumar, N. W. Emanetoglu, and Y. Lu, *Appl. Phys. Lett.* **80**, 2132 (2002).
- ²⁶H. von Wenckstern, G. Biehne, R. A. Rahman, H. Hochmuth, M. Lorenz, and M. Grundmann, *Appl. Phys. Lett.* **88**, 092102 (2006).
- ²⁷D. K. Schroder, *Semiconductor Material and Device Characterization* (Wiley, New York, 1998).
- ²⁸S.-H. Kim, H.-K. Kim, and T.-Y. Seong, *Appl. Phys. Lett.* **86**, 022101 (2005).
- ²⁹Y. M. Strzhemechny *et al.*, *Appl. Phys. Lett.* **84**, 2545 (2004).
- ³⁰Z.-Q. Fang, B. Claffin, D. C. Look, Y. Dong, and L. J. Brillson, *J. Vac. Sci. Technol. B* (in press).
- ³¹M. G. Wardle, J. P. Goss, and P. R. Briddon, *Phys. Rev. Lett.* **96**, 205504 (2006).
- ³²A. Janotti and C. G. Van de Walle, *Phys. Rev. B* **76**, 165202 (2007).
- ³³D. C. Oh, T. Kato, H. Goto, S. H. Park, T. Hanada, T. Yao, and J. J. Kim, *Appl. Phys. Lett.* **93**, 241907 (2008).
- ³⁴D. C. Look, B. Claffin, and H. E. Smith, *Appl. Phys. Lett.* **92**, 122108 (2008).